AGU PUBLICATIONS

JGR

Journal of Geophysical Research: Biogeosciences

RESEARCH ARTICLE
10.1002/2013JG002492

Key Points:
- Physical, chemical, and spectroscopic properties of bog peat were characterized

Correspondence to:
M. M. Tfaily,
malak.m.tfaily@gmail.com

Citation:
Tfaily, M. M., W. T. Cooper, J. E. Kostka, P. R. Chanton, C. W. Schadt, P. J. Hanson, C. M. Iversen, and J. P. Chanton (2014), Organic matter transformation in the peat column at Marcell Experimental Forest: Humification and vertical stratification, *J. Geophys. Res. Biogeosci.*, *119*, 661–675, doi:10.1002/2013JG002492.

Received 26 AUG 2013
Accepted 15 MAR 2014
Accepted article online 28 MAR 2014
Published online 28 APR 2014

Organic matter transformation in the peat column at Marcell Experimental Forest: Humification and vertical stratification

Malak M. Tfaily[1,6], William T. Cooper[2], Joel E. Kostka[3], Patrick R. Chanton[3], Christopher W. Schadt[4], Paul J. Hanson[5], Colleen M. Iversen[5], and Jeffrey P. Chanton[1]

[1]Department of Earth, Ocean and Atmospheric Science, Florida State University, Tallahassee, Florida, USA, [2]Department of Chemistry and Biochemistry, Florida State University, Tallahassee, Florida, USA, [3]School of Biology and School of Earth and Atmospheric Sciences, Georgia Institute of Technology, Atlanta, Georgia, USA, [4]Biosciences Division and Climate Change Science Institute, Oak Ridge National Laboratory, Oak Ridge, Tennessee, USA, [5]Environmental Sciences Division and Climate Change Science Institute, Oak Ridge National Laboratory, Oak Ridge, Tennessee, USA, [6]Pacific Northwest National Laboratory, Richland, Washington, USA

Abstract We characterized peat decomposition at the Marcell Experimental Forest (MEF), Minnesota, USA, to a depth of 2 m to ascertain the underlying chemical changes using Fourier transform infrared (FT IR) and ^{13}C nuclear magnetic resonance (NMR) spectroscopy) and related these changes to decomposition proxies C:N ratio, $\delta^{13}C$ and $\delta^{15}N$, bulk density, and water content. FT IR determined that peat humification increased rapidly between 30 and 75 cm, indicating a highly reactive intermediate-depth zone consistent with changes in C:N ratio, $\delta^{13}C$ and $\delta^{15}N$, bulk density, and water content. Peat decomposition at the MEF, especially in the intermediate-depth zone, is mainly characterized by preferential utilization of O-alkyl-C, carboxyl-C, and other oxygenated functionalities with a concomitant increase in the abundance of alkyl- and nitrogen-containing compounds. Below 75 cm, less change was observed but aromatic functionalities and lignin accumulated with depth. Significant correlations with humification indices, identified by FT IR spectroscopy, were found for C:N ratios. Incubation studies at 22°C revealed the highest methane production rates, greatest CH_4:CO_2 production ratios, and significant O-alkyl-C utilization within this 30 and 75 cm zone. Oxygen-containing functionalities, especially O-alkyl-C, appear to serve as excellent proxies for soil decomposition rate and should be a sensitive indicator of the response of the solid phase peat to increased temperatures caused by climate change and the field study manipulations that are planned to occur at this site. Radiocarbon signatures of microbial respiration products in deeper pore waters at the MEF resembled the signatures of more modern dissolved organic carbon rather than solid phase peat, indicating that recently photosynthesized organic matter fueled the bulk of subsurface microbial respiration. These results indicate that carbon cycling at depth at the MEF is not isolated from surface processes.

1. Introduction

Globally, peatlands sequester one third of all terrestrial soil carbon (C) and act as major sinks of atmospheric CO_2 [*Christensen et al.,* 1997; *Turunen et al.*, 2002; *Holden*, 2005]. The greatest concentration of peatlands, and the highest rates of peat formation, occurs in the cool, humid climates of the boreal Northern hemisphere [*Turunen et al.*, 2002; *Christensen et al.,* 2003]. This area is estimated to contain around 270–370 Gt of C as peat [*Turunen et al.*, 2002]. Long-term accumulation of peat in boreal peatlands occurs because productivity exceeds decomposition, which is a result of low pH, low temperatures, anoxia, inhibitory compounds inherent in the biomass of *Sphagnum* mosses, and chemically complex substrates with generally low nutrient content [*Freeman et al.*, 2001; *Moore and Basiliko*, 2006]. Climatic change, including rising atmospheric CO_2, warming, and changes in precipitation patterns, has the potential to alter the C balance of these systems. In particular, predicted increases in air and soil temperature may increase vegetation productivity and stimulate peat decomposition, and the resulting changes in peatland C balance have implications for feedbacks of CO_2 to the atmosphere.

Large-scale field experiments that simultaneously manipulate multiple climate factors are invaluable for quantifying the effects of atmospheric and climatic change on ecosystem processes and for providing information for large-scale models projecting future climates. At the Marcell Experimental Forest (MEF) near Grand Rapids Minnesota, USA, the U.S. Department of Energy's Oak Ridge National Laboratory and the U.S.

Forest Service are constructing a large-scale ecosystem study entitled, "Spruce and Peatland Responses Under Climatic and Environmental Change" (SPRUCE http://mnspruce.ornl.gov/). In this manipulation, large (12 m diameter) chambers will be used to assess the response of an ombrotrophic bog with an overstory dominated by black spruce (*Picea mariana* L.) trees to a range of air and soil temperatures, alone and in combination with elevated CO_2 concentrations.

The overall goal of this study is to focus on the aspects of the ombrotrophic bog that have the potential for change, including the physical, chemical, and spectroscopic properties of solid phase peat, which at the study site consists entirely of organic matter to a depth of greater than 2 m. It is important to note that the main goal of this work is not to test how these decomposition proxies are likely to respond to changes in temperature and climate perturbations but rather to characterize these indicators to better constrain soil organic matter (SOM) cycling, before the SPRUCE experiment starts. In particular, our goal is to determine specific chemical changes associated with peat decomposition at the S1 bog at the MEF.

SOM (soil organic matter) is a heterogeneous system that consists of plant and microbial residues in various stages of decomposition, living microorganisms, and substances synthesized microbiologically and/or chemically from decomposition products [*Schnitzer*, 1991]. The response of peatland SOM to climate warming is dependent upon the interactions between plant species composition and physiology, litter input, soil properties, and microbial decomposition processes [*Sjögersten et al.*, 2003]. Classifying total SOM into components with different biological and chemical availabilities is necessary to clarify the mechanisms of SOM formation, decomposition, and transformation [*Koarashi et al.*, 2005] and hence understand its potential response to environmental warming.

Peat can be divided by depth into two layers or subunits: the acrotelm, predominantly oxic, characterized with a high hydraulic conductivity and fluctuating water table and dominated by living plants and their roots, and the catotelm, an inert anoxic lower layer that corresponds to the permanently saturated main body of peat and where organic matter is mostly and stored [*Clymo,* 1984]. This layer represents the C "bank" of peatlands, as decomposition is limited due to saturated, anoxic conditions. *Clymo and Bryant* [2008] identified an additional layer, the usually anoxic but periodically oxic mesotelm that often coincides with the upper boundary of a fluctuating water table, as the transition zone between surface acrotelm and deep catotelm. This layer is characterized by fast anoxic decomposition and rapid carbon turnover. Peat physical and chemical properties reflect the environment under which the peat was formed, the processes leading to the development of the peat, and the composition of the plant community contributing to the buildup of organic matter. Physical properties of peat include the degree of decomposition, water content, and bulk density. Humification, a measure of the extent to which fresh organic matter has been transformed into recalcitrant humic substances [*Klavins et al.*, 2008], is one way to characterize the degree of peat decomposition. One of the important factors for organic matter (OM) decomposability is its chemical composition, which controls degradability, through the different activation energies associated with the various chemical bonds or OM qualities [*Conant et al.*, 2011; *Lützow et al.*, 2006].

During decomposition, organic C and organic nitrogen (N) content typically increase, whereas organically bound oxygen and hydrogen decrease [*Damman*, 1988; *Ekono*, 1981]. But as C compounds are consumed in peat, there is no inert mineral material to increase in relative concentration, so the remaining material increases in C content even as C is lost. N content can vary between 0.3% (by weight) in slightly decomposed peat and 4% in highly decomposed peat. Nitrogen abundance increases during decomposition when N is immobilized in microbial biomass [*Damman*, 1988] as soil microbes accumulate nutrients from the both decomposition products and the surrounding soil. Also, a fraction of the substrate is converted to fulvic and humic compounds that have high N content and long-term stability in the soil profile [*Aber and Melillo*, 1980; *Jackson et al.*, 1989]. Furthermore, peat N content varies depending on surface vegetation; peats developed from sedges, and reeds are usually 2 to 4 times higher in N than those formed from *Sphagnum* mosses [*Lucas*, 1982].

Isotope ratios have also been used as an indicator of decomposition processes; changes are assumed to reflect preferential utilization of ^{12}C by microbial processing of organic matter [*Kalbitz et al.*, 2000; *Hornibrook et al.*, 1997; *Keough et al.*, 1998]. Humified organic matter is ^{15}N- and ^{13}C-enriched compared to recent fresh organic compounds [*Kramer et al.*, 2003]. Stable C isotope compositions and the chemical composition of organic matter gradually evolve during degradation as different biochemical constituents are preferentially consumed, produced, or sequestered [*Benner et al.*, 1987].

Until recently, pore water flow through the deep anaerobic portion of a peat column (the catotelm) was considered negligible [*Clymo*, 1984; *Siegel et al.*, 1995]. The only input of organic matter was assumed to occur at the surface (the acrotelm), with no significant additional import of either dissolved organic (DOC) or inorganic carbon (DIC) to the catotelm. Therefore, microbial respiration within the catotelm was generally considered to be restricted to the degradation of the peat itself. However, *Chanton et al.* [2008] and *Chasar et al.* [2000] have more recently reported that anaerobic respiration within the peat column to depths of 3 m was fueled by DOC derived in part from surface processes rather than from the decomposition of deeper peat [see also *Aravena et al.*, 1993; *Chanton et al.*, 1995; *Charman et al.*, 1994, 1999; *Chasar et al.*, 2000; *Clymo and Bryant*, 2008; *Corbett et al.*, 2013b]. This finding was supported by differences in radiocarbon enrichment of DOC, and the products of anaerobic respiration (CO_2 and CH_4) relative to the solid peat in deeper horizons. These observations suggested that hydrology and surface vegetation can play an important role in belowground C cycling within peatlands.

Peat-forming plants contain high percentages of carbohydrates (O-alkyl-C), primarily as cellulose, that are readily degraded in soils [*Hopkins et al.*, 1997]. The degradation of labile plant-derived compounds increases the formation of non-O alkyls from two sources: (1) metabolic products of decomposer organisms and/or (2) transformation of the original O-alkyl-C to more recalcitrant forms [*Baldock and Preston*, 1995; *Hopkins et al.*, 1997]. Plants, especially mosses (e.g., *Sphagnum* that blankets the surface of ombrotrophic bog ecosystems), are a source of phenolics and aromatics in the soil that are known to be refractory [*Williams and Yavitt*, 2003].

Fourier transform infrared (FT IR) spectroscopy has been widely used to characterize organic matter quality of bulk peat as well as of humic and fulvic acids [*Holmgren and Nordén*, 1988] and provides information on the principal chemical classes in soil organic matter. FT IR can distinguish and quantitate compound classes such as carbohydrates, lignin, cellulose, fats and/or lipids, and proteinaceous compounds through the vibrational characteristics of their chemical bonds. FT IR has also been used recently to identify humification processes [*Broder et al.*, 2012] and describe the degree of decomposition through a series of humification indices that follow the reduction of carbohydrates (O-alkly-C) with depth [*Chapman et al.*, 2001].

Nuclear magnetic resonance spectroscopy over the last three decades has provided key insight into structural details of soil organic matter, including humic substances [*Preston*, 1996]. Solid state ^{13}C NMR was first applied to soil organic matter (SOM) in 1980 [*Wilson et al.*, 1981]. Since then, there have been many applications of ^{13}C NMR in studies of plant litter, organic wastes, whole soils and their fractions [*Baldock et al.*, 1997; *Fründ et al.*, 1994; *Preston*, 1996; *Preston et al.*, 1990], and to a lesser extent on peat organic matter and the changes in its composition with depth and across different sites [*Hertkorn et al.*, 2002; *Leifeld et al.*, 2012; *Segnini et al.*, 2013].

For this study, we utilized a combination of techniques, including Fourier transform infrared (FT IR) spectroscopy, ^{13}C NMR spectroscopy, C:N ratios of soil organic matter, ^{13}C and ^{15}N isotopes in the peat, ^{14}C of peat, dissolved inorganic carbon (DIC), and dissolved organic carbon (DOC) to relate decomposition processes at the MEF with the chemical changes that underlie these processes. Laboratory incubation studies of peat substrates were also used to relate peat chemical properties and with carbon dioxide and methane gas production. The specific objectives of this study were therefore (i) to use proxies to identify decomposition patterns at the MEF and relate them to underlying chemical changes; (ii) to elucidate the role of hydrology and surface vegetation in belowground carbon cycling at the S1 bog through the use of ^{14}C of DIC, DOC, and peat; and (iii) to test the hypothesis that that O-alkyl-C abundance will be a sensitive indicator of future perturbations to the system. This hypothesis was tested by conducting incubation studies at 22°C to quantify changes in peat chemical properties associated with carbon gas production.

2. Materials and Methods

2.1. Site Location

The SPRUCE experimental site is the S1 bog (8.1 ha) within the Marcell Experimental Forest (MEF; N 47°30.476′; W 93°27.162′), approximately 40 km north of Grand Rapids, Minnesota, USA [*Kolka*, 2011] http://mnspruce.ornl.gov/). Extensive scientific investigations have been conducted at this site for several decades [*Nichols and Brown*, 1980; *Urban et al.*, 1989; *Verry*, 1981].

Within the S1 bog, the overstory vegetation consists of two dominant tree species, black spruce *(Picea mariana)* and larch *(Larix laricina)*. The bog surface is characterized by hummock and hollow microtopography, with a

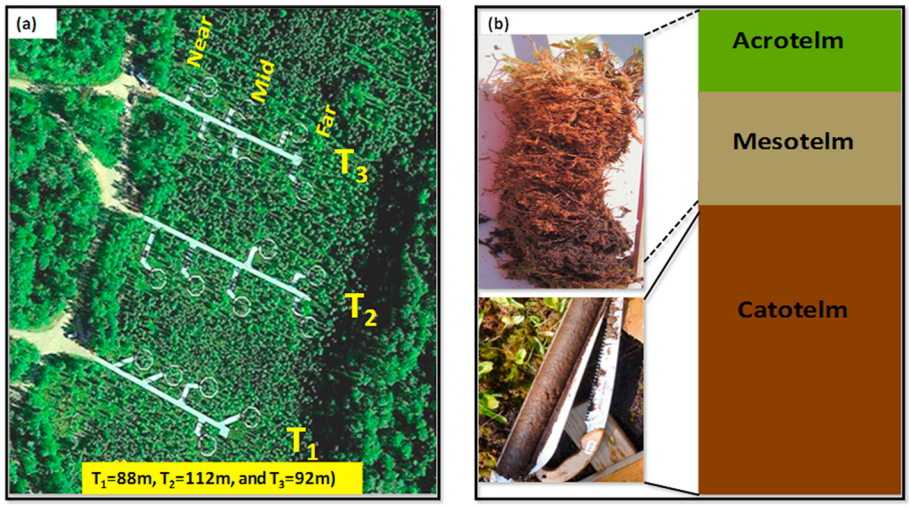

Figure 1. (a) An Oak Ridge National Laboratory aerial photograph of the S1 bog and three sampling transects. (b) Schematic diagram of a peat core collected from the S1 bog showing the three different zones identified in this study.

typical relief of 10 to 30 cm between the tops of the hummocks and the tops of the hollows. The bryophytes in hummocks consisted mainly of *Sphagnum magellanicum,* while hollows are mainly colonized by *S. angustifolium.* The understory consists mainly of ericaceous shrubs, including evergreen shrubs, as well as the deciduous common blueberry *Vaccinium angustifolium*. Sedges are relatively sparse compared with *Sphagnum* mosses and woody trees and shrubs. The common forb *Smilacina trifolia* (three-leaved false Solomon's seal) also appears sporadically, as do various other less common species.

2.2. Sampling

The S1 bog was divided into three transects (T_1, T_2, and T_3; Figure 1a). The approximate dimension for each transect was as follows: $T_1 = 88$ m, $T_2 = 112$ m, and $T_3 = 92$ m. For this study, three experimental plot centers, within each transect were chosen—Near (N), Mid (M), and Far (F)—from west to east across the bog (Figure 1a). Sample sites were labeled based on transect and plot, e.g., T_1F = the far plot along transect 1. In February of 2012, two cores (M and F) were collected from each transect for a total of six cores. All cores were collected in hollow microtopography, where the surface of the hollow was defined as 0 cm.

Surface peat (0–50 cm) was collected using a modified hole saw, while deeper peat (50–200 cm) was collected using a Russian peat corer. Once collected, the cores were sectioned into 10 cm increments in shallower peat and 25 cm intervals from 0.5 to 2 m, and the sections were placed into plastic bags and stored frozen at −20°C. Each section from each core was analyzed in duplicate for chemical and spectroscopic properties, and the average was reported. Surface samples up to 15–20 cm consisted of living and senesced *Sphagnum,* samples between 20 to 50 cm consisted of decomposing *Sphagnum* (decomposing moss litter), and deeper samples consisted of well-humified peat (Figure 1b).

In July of 2012, replicate cores were again collected from each of the three transects. Triplicate cores were also collected from an additional site called Environmental Monitoring Station number 2 site located at the southern end of the S1 bog. All samples from each core were analyzed individually, and the average was reported in this study. At this time, the water table at the S1 bog ranged between 0 and 10 cm below the surface of peat. In February of 2012, the S1 bog was covered with snow and the upper 25 cm below the surface of the peat was completely frozen. Based on these observations, the water table was assumed not to differ between July and February sampling trips as well as between the three transects.

Pore water samples were collected in July 2012 from two locations across transect 3 (Mid: T_3M and Far: T_3F). A peristaltic pump with Teflon tubing was used to collect pore water from 1.25 cm diameter PVC piezometers at ~25 cm depth intervals below the water table, which was at the surface of the hollows in July 2012 [*Corbett et al.*, 2013a]. Pore water samples were filtered through 0.7 μm glass fiber filters (Whatman) immediately after collection and stored frozen until time of analysis.

Table 1. Chemistry and Isotopic Signatures of Vegetation in the S1 Bog[a]

Vegetation	C (%)	N (%)	C:N	$\delta^{13}C$	$\delta^{15}N$
Sphagnum angustifolium					
Capitulum (3)	43.9 ± 0.2	1.2 ± 0.1	38.0 ± 3.1	−28.6 ± 0.3 (4)	−2.0 ± 0.4 (4)
Stem (3)	43.6 ± 0.3	0.9 ± 0.1	51.4 ± 4.8		
Sphagnum magellanicum					
Capitulum (3)	43.4 ± 0.6	1.2 ± 0.1	37.6 ± 0.8	−28.6 ± 0.3 (4)	−2.0 ± 0.4 (4)
Stem (3)	43.0 ± 1.0	0.8 ± 0.1	53.8 ± 1.3		
Picea mariana					
Leaves (3)	51.0 ± 0.2	0.7 ± 0.1	71.8 ± 2.2		
Fine roots (3)	52.9 ± 1.6	1.3 ± 0.1	48.5 ± 7.2		
Larix laricina					
Leaves (3)	51.0 ± 0.2	0.8 ± 0.1	64.2 ± 8.9	−31.3 ± 0.1 (3)	−6.5 ± 0.1 (3)
Fine roots (3)	54.2 ± 1.7	1.0 ± 0.1	56.7 ± 3.2		
Chamaedaphne calyculata					
Leaves (12)	53.1 ± 0.2	1.6 ± 0.1	33.4 ± 0.6		
Fine roots (4)	55.0 ± 2.3	0.8 ± 0.1	76.2 ± 13.9		
Ledum groenlandicum					
Leaves (14)	53.2 ± 0.2	1.3 ± 0.1	41.8 ± 0.6	−28.3 ± 0.1 (9)	−4.8 ± 0.2 (9)
Fine roots (2)	51.8 ± 3.3	1.2 ± 0.1	49.5 ± 6.4		
Kalmia polifolia					
Leaves (5)	52.6 ± 0.4	1.6 ± 0.1	33.6 ± 0.2	−30.6 ± 0.1 (3)	−5.3 ± 0.3 (3)
Smilacina trifolia					
Leaves (12)	49.6 ± 0.2	2.5 ± 0.1	20.7 ± 0.9	−28.3 ± 0.1 (3)	0.3 ± 0.1 (3)
Eriophorum spissum					
Leaves (10)	47.1 ± 0.2	1.5 ± 0.1	32.1 ± 0.2	−28.0 ± 0.1 (3)	−1.0 ± 0.2 (3)

[a]Data are mean ± 1 standard error, where number in parentheses indicates number of samples (*n* in parentheses) (C. T. Garten et al., unpublished data, 2010–2012).

In 2012, aboveground vegetation was sampled from experimental plots located across three transects in the S1 bog in order to determine the C and N contents of different plant species and tissues for current year growth. Aboveground data are the means of up to 14 plots ± 1 standard error, and the number in parentheses (Table 1) after species name indicates the number of plots represented. *Sphagnum* mosses and fine roots were also sampled in 2011 from voucher specimens collected along transects 1 and 2. *Sphagnum* C and N are given for both the green tops (capitula) and the top 4 cm of the stem (Table 1). Root C and N are given for small-diameter roots with short life spans (average diameter was less than 0.5 mm). For vascular plants, we only included data on leaves and fine roots here given the long turnover times of wood. In a prior year (2010), less extensive sampling was undertaken for isotopic analysis of vascular tissue, where old and new tissues were combined (though data are reported in the table as old tissue), and *Sphagnum* moss was not differentiated into species.

2.3. Peat Sample Preparation and Analysis of Bulk Physical and Chemical Properties

Peat sections were weighed, freeze dried, reweighed, and ground to a fine powder. Bulk density was calculated using the freeze-dried weights of the volumetric slices. Water contents were calculated as the total amount of water in the peat. Organic C and N concentrations were analyzed by combustion to CO_2 and N_2 at 1020°C in an automated CHN elemental analyzer coupled with a ThermoFinnegan Delta XP isotope ratio mass spectrometer for the determination of the stable isotope ratios of C ($\delta^{13}C$) and N ($\delta^{15}N$). Peat C:N ratios were calculated as weight ratios for corresponding samples. Samples were run in duplicate, and the average was reported.

For surface vegetation samples (Table 1), C and N contents of vegetation tissue were determined on oven-dried samples using an elemental analyzer (LECO TruSpec, LECO Corporation, St. Joseph, MI, for leaves or

Costech Analytical Technologies, Inc., Valencia, CA, for moss and roots), while the natural abundance of $\delta^{13}C$ and $\delta^{15}N$ were determined on oven-dried samples using an isotope ratio mass spectrometer (Integra CN, SerCon Ltd, Crewe, UK).

2.4. Spectroscopic Analyses

2.4.1. FT-IR Spectroscopy

Spectral characterization of peat samples was performed by diamond-attenuated total reflectance FT-IR spectroscopy using a PerkinElmer Spectrum 100 FT-IR spectrometer fitted with a CsI beam splitter and a deuterated triglycine sulfate detector. An attenuated total reflectance (ATR) accessory made from a composite of zinc selenide (ZnSe) and diamond, with a single reflectance system, was used to produce transmission-like spectra. Dried and ground peat samples from different cores/depths were placed directly on the crystal, and force was applied to ensure good contact between the crystal and the sample. Spectra were acquired by averaging 50 scans at 4 cm^{-1} resolution (wave number) over the range 4000–650 cm^{-1}. The spectra were corrected for the ATR to allow for differences in depth of beam penetration at different wavelengths and then baseline corrected with the instrument software.

2.4.2. ^{13}C NMR

Solid state cross-polarization magic angle spinning ^{13}C spectra were acquired with high-power proton decoupling on a Bruker Unity-Inova 500 MHz spectrometer operating at 125 MHz for C. Depending on the density of the sample, approximately 500 mg of the dried peat were packed into a 7 mm (outside diameter) solid state rotor with a Kel-F cap and spun at 5 kHz. Spinning sidebands were eliminated using the total suppression of sidebands sequence. Between 32,000 and 45,000 scans were accumulated using a 90° pulse of 6.5 μs pulse width, 750 μs cross-polarization contact time, and a 3 s pulse delay. This contact time may have underestimated fast-rotating alkyl functional groups, but previous experiments on similar wetland soils suggest that more than 95% of soil C is "observable" using these parameters [*Hamdan et al.*, 2012]. Chemical shifts were externally referenced to the 41.5 ppm resonance of glycine. The relative distribution of C groups in different structures was determined by integrating the signal intensities over defined chemical shift windows. These spectral windows and the structures they represent were 0–50 ppm (alkyl-C), 50–110 ppm (O-alkyl-C), 110–160 ppm (aromatic-C), and 160–220 ppm (carbonyl-C found in carboxylic acids, esters, amides, ketones, and aldehydes).

2.5. Radiocarbon

The preparation of $\Delta^{14}C$-DOC, $\Delta^{14}C$-DIC, and $\Delta^{14}C$-peat samples was done at the National High Magnetic Laboratory at Florida State University following the methods described in *Corbett et al.* [2013b]. Following cryogenic purification, the resultant CO_2 was sent for $\Delta^{14}C$ analysis to the National Ocean Sciences Accelerator Mass Spectrometry Facility.

2.6. Peat Incubations

Approximately 20 g of defrosted peat from selected depths (0–10 cm, 20–30 cm, 75–100 cm, and 175–200 cm) from the July 2012 collection of peat from the T_3M site at S1 were added to preweighed 125 mL vials. Twenty milliliters of anoxic Milli-Q water was then added to the vials to make peat slurry. Each vial was sealed and flushed with N_2 gas for 30 min and shaken by hand. Duplicate incubations were done by placing peat from the same depth into separate incubation jars. The vials were preincubated for 2 weeks at 22°C in the dark. The vials were then flushed with N_2 gas and incubated at 22°C in the dark for 75 days. Measurements for gas concentration (CH_4 and CO_2) and isotopic ratio were conducted on a gas chromatography-combustion interfaced-isotope ratio mass spectrometer (Finnegan MAT Delta V GC-IRMS). Because CO_2 is highly soluble in water, 1 mL of 43% H_3PO_4 was added to each incubation vial at the end of the incubations. The vials were shaken, left to sit for 1 h, and shaken again. Subsamples from the headspace were measured on the GC-IRMS to account for any additional CO_2 from DIC. The acid addition did not significantly change the concentration of the CO_2 in the headspace, suggesting most of the CO_2 remained concentrated in the headspace throughout the study.

2.7. Incubation Calculations

The headspace mole fractions of CH_4 and CO_2 obtained from the GC-IRMS were converted to molar amounts of CH_4 and CO_2 in the whole vial. CH_4 and CO_2 production rates were calculated based on linear regressions

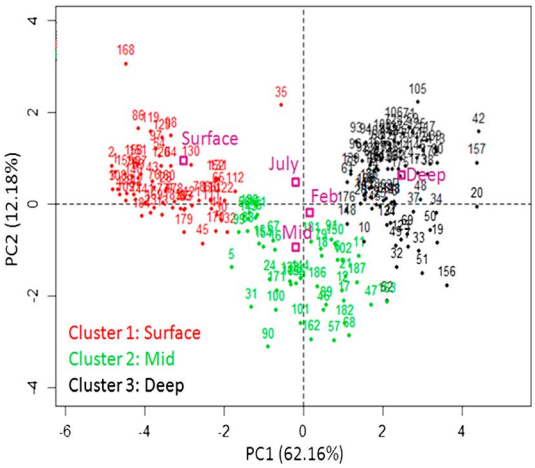

Figure 2. Principal coordinate analysis of the different peat physical and spectroscopic parameters comparing similarity among the data collected during February and July sampling trips and across the three different zones within the peat profile (Surface, Mid, and Deep). PC1 correlated positively with humification indices, %C, %N, and δ^{13}C and negatively with % water content and C:N ratios. PC2 correlated positively with dry bulk density and δ^{15}N.

of molar amount versus time up to day 75, and the slopes were divided by the mass of dry peat in each vial and averaged for all replicate vials.

3. Results and Discussion

3.1. Enhanced Peat Decomposition at the Mesotelm Layer

We compared specific chemical changes associated with peat decomposition across three different zones within the peat column (Figure 1b) at the S1 bog using C:N ratios, bulk density, FT IR, and NMR spectroscopy, humification indices and δ^{13}C and δ^{15}N isotopic signatures. Principal component analysis of the different decomposition proxies (Figure 2) revealed significant differences among the three peat zones but only minor differences across seasons (February versus July). Most of the variance (62%) was explained by the first component (PC1), whereas 12% of the variation was explained by the second component. Surface peat samples (Zone 1 samples) were separated from deep samples (Zone 3) through PC1, which correlated positively with humification indices, %C, %N, and δ^{13}C and negatively with % water content and C:N ratios. Intermediate depth samples (Zone 2) were separated from surface and deep peat samples across PC2. PC2 correlated positively with dry bulk density and δ^{15}N.

The acrotelm (Zone 1) extended to around 30 cm below the peat surface and consisted of living mosses and their newly formed litter, in addition to root material. Peat in the acrotelm was characterized by low decomposition rates. This observation was based on the low bulk density (0.04–0.12 g cm^{-3}; Figure 3a), high water content (87–95%; Figure 3b), high C:N ratios (35–50; Figure 3c) and low %C and %N, respectively (40–45% and 1–1.5%; Figures 3d and 3e). The high C:N ratios observed for surface samples were expected as they contained fresh and poorly decomposed *Sphagnum* (Table 1). These results are consistent with *Sphagnum* having low N content compared to the vascular plants in the S1 bog (Table 1), though *Sphagnum* litter does decompose, albeit slowly when compared with vascular litter [*Asada et al.*, 2005; *Clymo*, 1984; *Limpens et al.*, 2008].

Stacked FT IR spectra as a function of depth are given in Figure 4. Spectra were characterized by a number of absorption bands, exhibiting variable relative intensities typical of humic-like materials [*Artz et al.*, 2008;

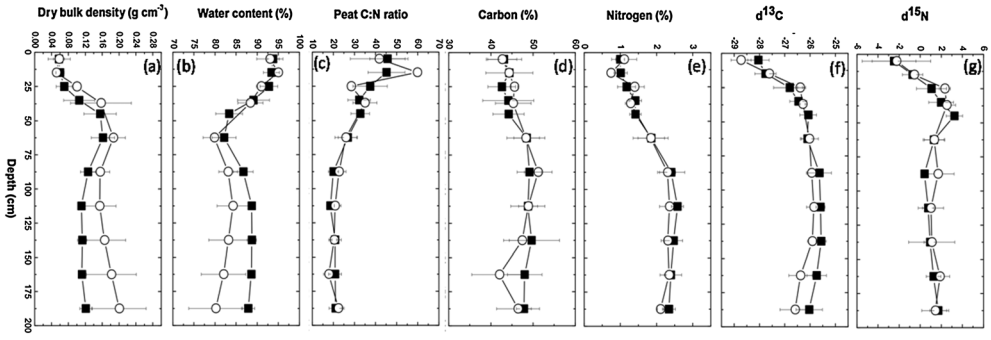

Figure 3. Physical and chemical properties of all peat cores collected from S1 bog of the Marcel experimental forest: (a) dry density in g cm^{-3}; (b) water content (%); (c) C:N of solid phase peat; (d) carbon (%) of solid peat; (e) nitrogen (%) of solid phase peat; (f) δ^{13}C of solid phase peat; and (g) δ^{15}N of solid phase peat. February 2012 (open circles); July 2012 (closed squares). February 2012 data $n = 6$; July 2012 data, $n = 14$.

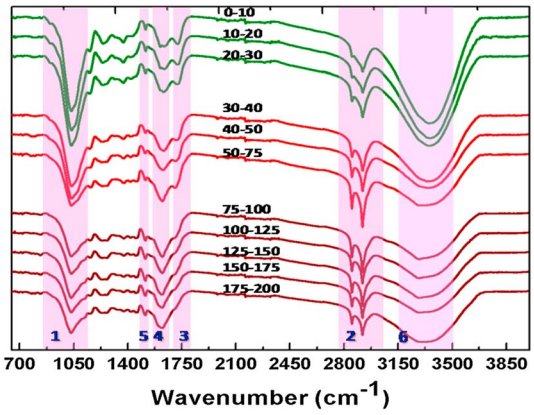

Figure 4. Average FT IR spectroscopy from 20 peat cores. Peak number 1 represents carbohydrates/cellulose/O-alkyl-C; peak number 2 represents aliphatics; peak number 3 represents organic acids; peak number 4 represents aromatic rings and C–O of quinine and amide groups; and peak number 5 represents lignin residues and aromatic functionalities. Spectra are stacked, and differences along the *y* axis are relative.

Chapman et al., 2001; *Leifeld et al.,* 2012]. Surface samples exhibited a low transmittance (high absorption) at the O-alkyl-C peak (peak number 1 at 1030 cm^{-1}), suggesting an abundance of O-alkyls (carbohydrates) at this depth. The peak occurring at 1735–1725 cm^{-1} (peak number 3; Figure 4), attributed to the C═O stretching of carbonyl functions (aldehydes and ketones), organic acids, and other oxygenated functionalities, was also evident and distinct in the first portion of the profile (0–20 cm). The broad absorption band occurring around 2900 cm^{-1} associated with asymmetric and symmetric C–H stretching of the CH_3 and CH_2 groups of aliphatic hydrocarbons (peak number 2) was relatively small at the surface compared to the deeper samples. In addition, the aromatic peak (peak number 4) occurring around 1610 cm^{-1} in the top layers, ascribed to C═C bonds of the aromatic rings and C–O of quinine and amide groups, was relatively small too, suggesting low abundance of aromatic compounds in the surface samples. The small peak occurring at 1515 cm^{-1} (peak number 5) reflects a low abundance of lignin-like residue at the surface compared to deeper samples, consistent with low levels of decomposition in the acrotelm [*Beer et al.*, 2008; *Broder et al.*, 2012; *Cocozza et al.*, 2003].

^{13}C NMR spectra were collected on representative samples in the T_3M core from the February 2012 sampling (Figure 5). Generally, the spectra showed similar characteristics, presenting signals that are associated with the different functional aliphatic (C–H, C–N, O–CH_3, O-alkyl-C) and aromatic (C-H and phenolic) groups. The observed peaks have been frequently reported by other researchers who have used ^{13}C NMR to study and characterize different types of organic matter [*Ahmad et al.*, 2001]. Generally, the O-alkyl-C (60–100 ppm region) dominated in the surface samples up to 30 cm, with the alkyl C (0–50 ppm region), the next quantitatively most important C type, followed by the aromatic C (110–160 ppm region).

The second layer, the mesotelm (30–75 cm), appears to be a transition zone between the largely oxic acrotelm and the anoxic catotelm. This zone was characterized by intense decomposition. Bulk density in the S1 bog

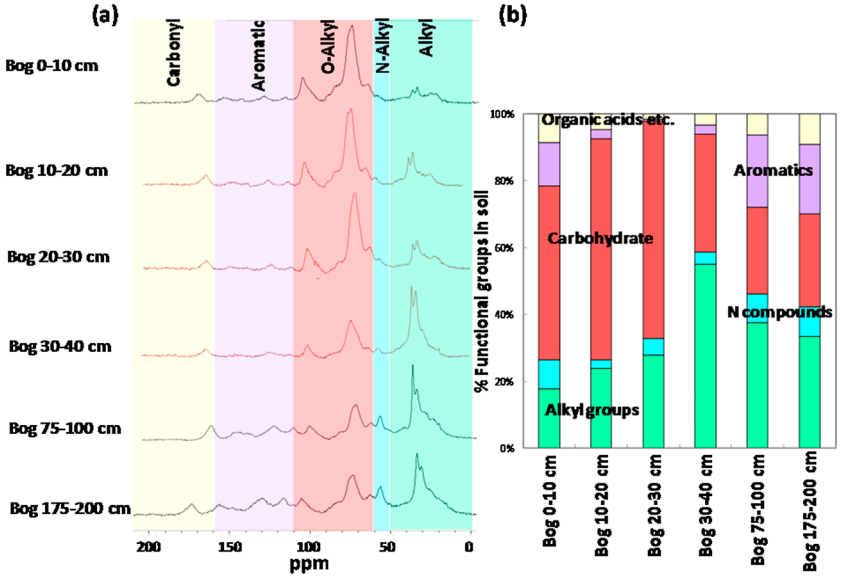

Figure 5. (a) ^{13}C NMR on selected samples from T_3M bog site; (b) functional groups (%) at each depth.

reached a maximum, with values up to nearly 3 times greater than overlying depths (Figure 3a), accompanied by a drop in % water content (80%), indicating that decomposition occurred more rapidly in this zone than in other layers. The phenomenon of strongly decomposed (humified) peat in mid-subsurface layers has been observed in Sweden [*Franzén*, 2006] and in the Jura Mountains of Switzerland [*Cocozza et al.*, 2003], though other studies suggest maximum humification and decomposition generally occur below 100 cm depth, in a more gradual progression from the surface [*Borgmark and Schoning*, 2006; *Broder et al.*, 2012]. In the S1 bog, water table fluctuations may be responsible for the increased decomposition between 30 and 75 cm via secondary decomposition of previously buried peat [*Borgmark and Schoning*, 2006; *Sebestyen et al.*, 2011]. Wet conditions trigger peat accumulation due to imbalance between litter inputs and decomposition rates, whereas dry periods may expose peat to aerobic decay and more rapid decomposition [*Broder et al.*, 2012].

Further evidence of intense decomposition at this layer comes from C:N ratios (Figure 3c). Peat C:N ratio declined once decomposing peat reached the intermediate-depth zone (30–75 cm). C:N ratios provide information about the state of organic matter decomposition and have been used as a general index of plant litter quality since the 1920s [*Waksman*, 1924]. A low C:N ratio is usually equivalent to a high humification degree [*Waksman*, 1924; *Waksman and Tenney*, 1927]. Peat N values increased sixfold, from 0.5% at the surface to 3% at 50 cm (Figure 3e). These values are similar to those reported in other studies [*Vardy et al.*, 2000]. Explanations for the increase in N with depth in our system, especially at the mid-depth zone, are twofold: N immobilization/retention in microbial biomass [*Damman*, 1988] and, in addition, the formation of fulvic and humic compounds that have high N content and long-term stability in the soil profile [*Aber and Melillo*, 1980; *Jackson et al.*, 1989].

Peat C values also increased with depth, from ~ 42% at 5 cm to ~50 % at 50 cm (Figure 3d). The increase in C content was, however, less significant when compared to the increase in nitrogen content (approximately sixfold), leading to decreased C:N ratios with depth. The increase in %C with depth in the peat profile is due to the fact that as C compounds are consumed, there is no inert mineral material to increase in relative concentration.

FT IR data were also consistent with intense decomposition at the mesotelm (Figure 4). The most pronounced change was that of the O-alkyl-C peak (peak number 1 at 1030 cm^{-1}), which decreased markedly between 30 and 75 cm, indicating significant O-alkyl-C (carbohydrate) consumption. The broad band at about 3400 cm^{-1} (peak number 6), generally ascribed to O–H stretching of hydrogen-bonded O–H groups, decreased to a minimum between 30 and 75 cm, following the pattern of peak number 1. The broad absorption band occurring around 2900 cm^{-1} associated with asymmetric and symmetric C–H stretching of the CH_3 and CH_2 groups of aliphatic hydrocarbons (peak number 2) differentiates markedly with depth starting at 30 cm into two separate and very distinct peaks at 2920 and 2850 cm^{-1}. This differentiation indicates extensive transformation of simpler aliphatic moieties and a marked increase and/or accumulation of refractory aliphatic components especially in the mid-depth zone [*Cocozza et al.*, 2003]. The peak occurring at 1735–1725 cm^{-1} (peak number 3; Figure 3), attributed to organic acids and other oxygenated functionalities, shifted to 1710 cm^{-1} (30–75 cm) at the mesotelm. In addition, the aromatic peak (peak number 4) occurring around 1610 cm^{-1} shifted toward 1650 cm^{-1} in the active layer and increases in intensity with depth along the peat core, suggesting an increase in the amount of aromatic residues with depth. Also, the small peak occurring at 1515 cm^{-1} (peak number 5), usually related to lignin-like residues, decreased in the transition zone [*Beer et al.*, 2008; *Broder et al.*, 2012; *Cocozza et al.*, 2003]. These results are consistent with the greatest rates of decomposition occurring at intermediate peat depths (Zone 2; Figure 1b), leading to the release of variable amounts of organic acids within this zone.

In the NMR data (Figure 5), a decrease in the O-alkyl-C signal (carbohydrates) and a relative increase in the alkyl, N-alkyl, and aromatic regions were observed at the 30–40 cm zone, consistent with the FT IR data. Most plant-derived compounds are O-alkyl-C in the form cellulose (complex carbohydrate) [*Kögel-Knabner*, 2000; *Leifeld et al.*, 2012]. The degradation of these and other oxygenated C compounds causes an increase in the relative abundance of alkyls, formed as metabolic products of decomposer organisms and/or through transformation of the original O-alkyl-C structures to more recalcitrant alkyl forms [*Baldock and Preston*, 1995; *Hopkins et al.*, 1997]. The lowest alkyl-to-O-alkyl ratio was observed at the surface.

Unlike FT IR, ^{13}C NMR allows for the differentiation between the two sources of alkyl groups formed at the mid-depth zone within the peat profile (Figure 5). Our ^{13}C NMR data show evidence of formation of alkyl groups from both processes. The formation of N-alkyls as metabolic products of decomposer organisms is

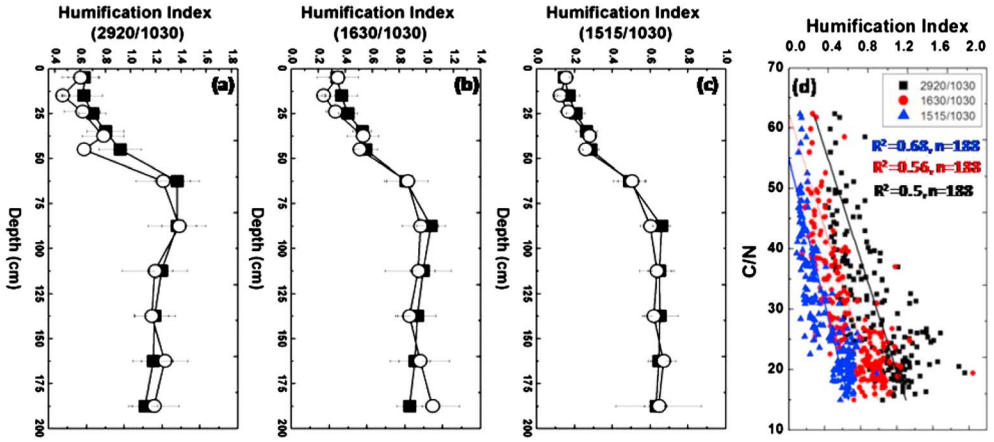

Figure 6. Average humification indices values, as identified by FT IR, versus depth (cm) at different depths during the summer (July) and winter (February) seasons (total of 20 peat cores). (a) Humification index calculated from 2920/1030 cm^{-1} (alkyl-C/O-alkyl-C). (b) Humification index calculated from 1630/1030 cm^{-1} (aromatic-C/O-alkyl-C-C). (c) Humification index calculated from 1515/1030 cm^{-1} (lignin residue/O-alkyl-C). February 2012 (open circles); July 2012 (closed squares). (d) C:N ratio versus humification indices.

indicated by the increase in relative abundance of N-alkyls at the mid-depth zone (Figure 5, blue shaded areas). N-alkyl groups could arise from the α C of amino acids, peptides, and proteins, hence reflecting microbial activity at this zone. The increase in the abundance of N-alkyl compounds at this zone could explain the increase in the % nitrogen in and below the active zone. Alkyl group formation at the mid-depth zone could also be the result of transformations of the original O-alkyl-C structures to more recalcitrant alkyl forms through the aid of the microbial communities that are striping the C–O bonds off the O-alkyl-C polymers to form refractory alkyl polymers rather than small molecule weight O-alkyl-C monomers (Figure 5, green bars).

The underlying third zone (below 75 cm depth), the catotelm, was more homogenous, with low decomposition rates compared to the mesotelm. The catotelm exhibited lower bulk density (and hence high water content; Figure 3) compared to the mesotelm but higher values compared to the acrotelm. C:N ratios, %C, and %N remained relatively constant below the meostelm, suggesting very slow decomposition at depth [*Kuhry and Vitt*, 1996; *Vardy et al.*, 2000]. Furthermore, the solid phase peat profile in the catotelm was characterized by relative stasis as reflected by the more homogenous spectroscopic line shapes of the peat samples (Figure 4). The intensity of the aliphatic peaks (2) decreases toward the lower portion of the core, indicating some consumption of aliphatic compounds with depth. Organic acid components decrease successively in intensity, appearing as a constant shoulder toward the lower portion of the peat core (100–200 cm). The % abundance of aromatic compounds was higher in the deeper samples, suggesting humification and accumulation of lignin-like aromatic residue with depth. Nonetheless, the data show that major changes in the functional groups occur in the mid-depth zone. Below the active zone, only slight changes in the abundance of the functional groups are observed, further indicating the homogenous nature and slow decomposition of the solid phase at depth. The consistency between FT IR (Figure 4) and ^{13}C NMR (Figure 5) data suggest that FT IR is a reliable technique for quantitative and qualitative analysis. In summary, our FT IR and ^{13}C NMR data suggest that the carbohydrates, carboxyl-C, and other oxygenated functionalities decline with depth, especially at the mid-depth zone (30–75 cm), whereas aliphatic-C, aromatic C, and microbial mucilage or nitrogen-containing compounds increase.

To relate peat C:N ratios and extent of humification and to quantitatively compare summer and winter seasons, the relative abundance of functional groups from FT IR data were used to calculate several humification indices. In particular, ratios between peak intensities for aliphatics (2920 cm^{-1}), aromatics (1630 cm^{-1}), and lignin residues (1515 cm^{-1}) with respect to polysaccharides (1030 cm^{-1}) were calculated [*Beer et al.*, 2008; *Broder et al.*, 2012; *Holmgren and Nordén*, 1988]. All ratios increased with depth (Figures 6a–6c), particularly at intermediate peat depths, indicating consumption of polysaccharides and increase in aromatic, amide, and phenolic moieties (from ~ 0.4 to 1.4 for aliphatics:carbohydrates; from ~0.2 to 1 for aromatics:carbohydrates; and from ~0.1 to 0.6 for lignin residue:carbohydrates). No seasonal variations in the humification values were observed upon

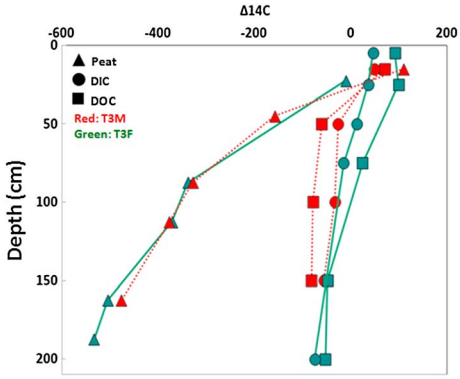

Figure 7. Radiocarbon values of peat (triangles), DIC (circles), and DOC (squares) collected from T_3M (red) and T_3F (green) in S1 bog.

comparing summer and winter samples (Figures 6a–6c), indicating that vertical stratification was more pronounced than temporal or lateral spatial differences. It is important to note that an increase in humification index values occurred at intermediate peat depths (Zone 2; Figure 1b) where the bulk of the decomposition occurred. Peat C:N ratios were inversely proportional to FT IR-derived humification indices (Figure 6d) ($r^2 = 0.5$ for aliphatics:carbohydrates, $r^2 = 0.56$ for aromatics:carbohydrates, and $r^2 = 0.68$ for lignin residue: carbohydrates; $n = 188$ (combined winter and summer samples)). The more humified the peat, the lower the C:N ratio. Similar patterns have been reported previously for northern temperate peatlands [*Borgmark and Schoning*, 2006; *Broder et al.*, 2012; *Lucas*, 1982]. *Borgmark and Schoning* [2006] investigated decomposition patterns in three cores collected from three ombrotrophic bogs and noticed a generally increasing humification index with depth at all three sites. Even though peat C:N ratios were negatively correlated to humification index, they were not correlated with depth and deviations of the two decomposition parameters (humification index and C:N) occurred as reported in the study of *Borgmark and Schoning* [2006].

Carbon and nitrogen isotope ratios (Figures 3f and 3g) help elucidate the pathways of organic matter degradation [*Dai et al.*, 2005; *Keough et al.*, 1998]. In this study our degradation continuum began with fresh *Sphagnum* and ended with deep peat from the 200 cm horizon. Organic matter became enriched in $\delta^{13}C$ with depth (Figure 3f) and increased from −28.4‰ (± 0.4 ‰, $n = 20$) at 5 cm to −25.9‰ (± 0.5 ‰, $n = 20$) at 187 cm (Figure 3g). These changes correlate well with the humification indices ($r^2 = 0.48$ for aliphatics: carbohydrates; $r^2 = 0.53$ for aromatics:carbohydrates; and $r^2 = 0.59$ for lignin residue:carbohydrates; $n = 188$) and C:N ratios ($r^2 = 0.55$, $n = 188$), indicating that decomposition has significantly altered the ^{13}C of surface vegetation [*Wang et al.*, 2008]. Of course, part of the change in the $\delta\ ^{13}C$ with depth could be due to the increase of ^{13}C depleted fossil carbon in the atmosphere [*Ghosh and Brand*, 2003]. Less humified samples (surface samples) had high C:N ratios, light $\delta^{13}C$ values, and low humification indices. With depth, C:N ratios and humification indices increased and peat $\delta^{13}C$ became enriched. Our FT IR and NMR data indicated compound-specific/selective decomposition [*Benner et al.*, 1987]; in particular, the relative amount of easily degradable carbohydrate compounds decreased with depth and the relative amount of lignin and aliphatic compounds increased. Compound-specific decomposition would therefore result in decreased $\delta^{13}C$ with depth and/or decomposition [*Benner et al.*, 1987]. Instead, peat $\delta^{13}C$ in our cores increased with decomposition. Kinetic fractionation against ^{13}C during decomposition and respiration may have caused such increase in $\delta\ ^{13}C$ in the residual material. However, this process is not fully understood. The observed changes in direction and magnitude of $\delta\ ^{13}C$ values are also consistent with a gradual shift in the relative contribution of microbial biomass as opposed to plant material [*Taylor et al.*, 2003].

$\delta^{15}N$ values increased with depth (Figure 3g) from −2.4 ‰ (±2‰, $n = 20$) at 5 cm to 1.6 ‰ (±1, $n = 20$) and did not consistently relate to any decomposition index and reached a maximum at intermediate peat depths, below which $\delta^{15}N$ decreased. Seasonal comparisons showed no significant change in $\delta^{15}N$ values. N isotopic composition is progressively enriched through the loss of more labile components and subsequent breakdown of proteins via degradation [*Dai et al.*, 2005]. This observation is consistent with our data where we observed maximum enrichment at the intermediate depth zone (Zone 2; Figure 1b), below which the $\delta^{15}N$ decreased but was still more enriched compared the surface samples (Zone 3; Figure 1b). Kinetic fractionation resulting from a number of processes including decomposition, nitrification, denitrification, and microbial incorporation of N may explain part of the enrichment in the deeper layers.

3.2. Carbon Cycling Processes at Depth are not Isolated From Surface Processes

Radiocarbon ($\Delta^{14}C$‰) measurements of the solid phase peat, dissolved inorganic C (DIC), and dissolved organic C (DOC) at two sites within the S1 bog (Figure 7) indicate that the majority of the microbial respiration occurring in the deeper peat is currently driven by surface photosynthetic production rather than peat decomposition.

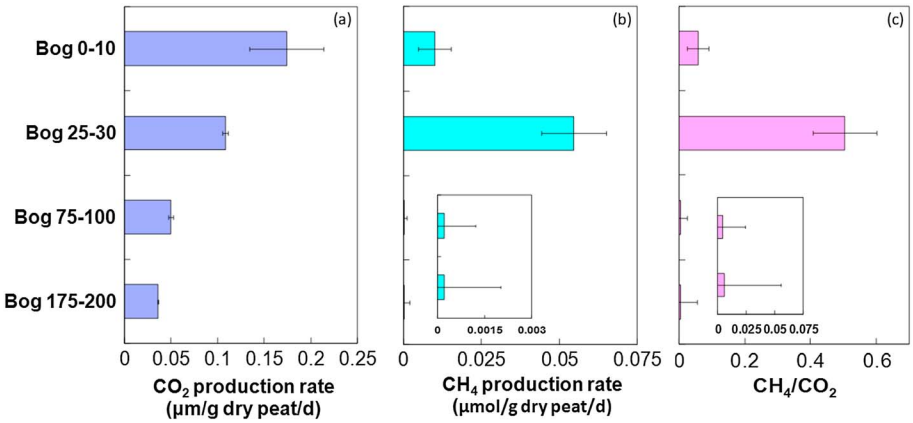

Figure 8. Production potential of (a) CO_2, (b) CH_4, and (c) CH_4/CO_2 from T_3M site. Values represent averages of duplicate incubations, and error bars represent relative error.

Negative values indicate older material, and at depth the peat (Figure 7, triangles) approaches 6000 years old (−600‰). The DOC (squares), which represents the remnants of plant and microbial biomass, varies from 40 to 100‰ at the surface, reflecting the values of recent photosynthetic production influenced by bomb testing in the 1960s–1970s. DOC is modern relative to the solid peat to a depth of 2 m, indicating that even at depth DOC input is dominated by surface production rather than from the decomposition of peat at a particular horizon.

DIC represents the signature of microbial respiration products. The $\Delta^{14}C$ values of DIC, representing the substrates utilized for microbial respiration, are more similar to the modern DOC values than they are to the peat, further reinforcing the interpretation of the relative stability of the catotelm solid phase peat under current climatic conditions. Similar findings have been reported for other peatlands [*Aravena et al.*, 1993; *Chanton et al.*, 2008; *Charman et al.*, 1994; *Clymo and Bryant*, 2008; *Corbett et al.*, 2013b]. The presence of labile DOC deeper in the peat column indicates that the S1 bog is hydrologically active with possible components from both vertical and lateral flow. Our radiocarbon data therefore suggest that (1) hydrology and surface vegetation play a role in belowground carbon cycling and that (2) that the lack of easily degradable carbohydrates in the deep peat and the presence of a fresh labile DOC source affect decomposition patterns. The deeper microbial communities appear to preferentially utilize the more modern labile DOC relative to the peat with its low carbohydrate abundance. This explains the stable humification index and lack of variation in $\delta^{13}C$, $\delta^{15}N$, and C:N ratios observed in the solid phase peat below the mid-depth zone. At the mid-depth zone, microbes appear to be utilizing both peat, which at that depth is richer in carbohydrates, and fresh labile DOC to produce respiration products that have a radiocarbon character in between peat and DOC (Figure 7).

3.3. O-Alkyl-C as a Proxy for Soil Decomposition Rate

We evaluated our hypothesis that the O-alkyl-C abundance will serve as a sensitive indicator of perturbations to the system in the incubation study described below. The highest CH_4 production rates were observed at intermediate peat depths, followed by a decrease in production rates in deeper peat (Figure 8). In contrast, CO_2 production rates were highest in surface peat and decreased with depth. The increase in CH_4 production at intermediate peat depths (Zone 2; Figure 1b), which occurred under identical temperature and conditions of water saturation, may be attributed to the higher level of labile organic C compounds, as indicated by FT IR and ^{13}C NMR. Little, if any, CH_4 was produced in deeper peat, which could be due to (1) the low lability of peat C present at this depth (i.e., low abundance of oxygenated functionalities), and/or (2) the accumulation of metabolic end products at depth produced within peat bogs that have been shown to inhibit microbial metabolism [*Williams and Crawford*, 1984], and/or (3) the lower initial population levels of methanogens and/or shifts in the methanogen community. *Williams and Crawford* [1984] found that methane production increased with increasing temperature, but markedly less increase with temperature was observed in peats from deeper layers. Since our incubations were conducted at a much higher temperature than normal field temperatures, the increase in the temperature, the composition of peat itself, and the high abundance of oxygenated functionalities (especially O-alkly-C) at intermediate peat depths could have enhanced microbial activity at this depth.

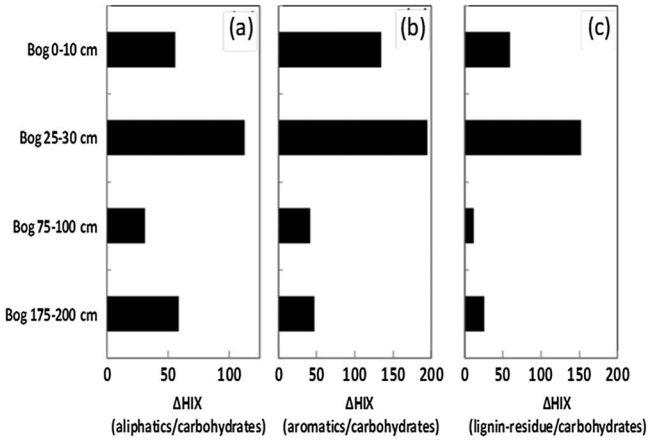

Figure 9. Change in humification indices values after incubation. (a) Change in the ratio of aliphatics with respect to carbohydrates; (b) change in the ratio of aromatics with respect to carbohydrates; and (c) change in the ratio of lignin residues with respect to carbohydrates.

FT IR spectra were also collected on the peat before and after incubation. Peat from intermediate depths showed the highest increase in humification values (Figure 9), consistent with high rates of microbial C mineralization and high CH_4 production. The humification increase was driven by a decline in O-alkyl-C abundance and an increase in alkly-C and was consistent with our hypothesis that O-alkyl-C abundance is sensitive to thermal perturbation. These results indicate that O-alkyl-C abundance could serve as a sensitive indicator for changes in C pools with warming [*Leifeld et al.,* 2012].

4. Conclusions

We characterized peat decomposition patterns and the underlying chemical changes in three zones within the peat profile at the S1 bog at the MEF. Decomposition proxies appeared to be influenced by both vegetation changes and decomposition, which are in return influenced by water table levels. All decomposition proxies showed mass loss and enrichment of more persistent compounds. The three zones were characterized as follows: the acrotelm, consisting of living *Sphagnum* mosses and their newly formed litter (0–30 cm), an intermediate depth transition zone characterized by rapid decomposition (30–75 cm), and the underlying catotelm where organic matter composition was fairly constant and diminished rates of solid phase peat decomposition were observed (below 75 cm; Figure 1). Multiple independent lines of evidence indicated that elevated decomposition in the intermediate depth transition zone resulted in changes to organic functional groups (i.e., loss of carbohydrates and increase in aliphatic and aromatic functional groups). Relative enrichment of ^{13}C in SOM with depth reflected a preferential loss of ^{12}C with decomposition. Enrichment of ^{15}N with depth, especially at the intermediate depth zone, and trends consistent with solid peat C:N ratios over depth suggested microbial recycling/immobilization of N. O-alkyl-C compounds were consumed in the active zone accompanied by accumulation of alkyl and N-alkyl groups. The abundance of O-alkyls, alkyls, and N-alkyls remained relatively constant in deeper horizons, although a slight decrease in their abundance in the deeper zone, combined with an increase in the abundance of aromatic compounds, indicated humification of the peat. Hydrology and surface vegetation played a role in belowground C cycling within the S1 bog by providing a modern labile source of C for microbial communities deep in the catotelm that is preferable to solid peat with low levels of easily biodegradable material (i.e., carbohydrates).

Collectively, our findings suggest that oxygen-containing functional groups, especially O-alkyl-C, may be of particular relevance for the decomposition of peat with warming and accompanying changes in the water table level in the SPRUCE experiment. Moreover, differences in the radiocarbon values of solid peat, DIC, and DOC indicated that microbial respiration at depth is currently fueled by surface inputs of DOC and further indicated that the decomposition of deeper solid phase peat will be readily observable in the ^{14}C signature of DIC if decomposition in deeper soil occurs in response to warming or elevated CO_2 treatments.

Our study represents a valuable baseline data set for the SPRUCE experiment, whose main objective is to assess the response of a northern peatland ecosystem to warming and elevated levels of atmospheric CO_2. We will be able track the effects of the experimental treatments on SOM decomposition processes throughout the peat profile by monitoring humification indices, abundance of functional groups, peat C:N ratios, as well as the $\delta^{13}C$ and $\delta^{15}N$ of peat and the $\Delta^{14}C$ of peat, DIC, and DOC.

Acknowledgments

We thank Randall Kolka, MN forest services, Xueju Lin, J. Megan Steinweg, and the rest of SPRUCE team for help with sample handling and providing laboratory space support. We thank Erik Hobbie for his valuable comments on the manuscript. Radiocarbon samples were run at the National Ocean Sciences Accelerator Mass Spectrometry Facility (NOSAMS). We thank Kathryn Elder, Sue Handwork, and Ann McNichol at NOSAMS for their expert work. We also would like to acknowledge Deanne Brice; Joanne Childs; Charles Garten, Jr.; Les Hook; Jana Phillips; Richard Norby; and David Weston for help with vegetation collection and processing. This work was supported by the Office of Biological and Environmental Research, Terrestrial Ecosystem Science Program, under U.S. DOE contract ER65245. The SPRUCE experiment is supported by the United States Department of Energy, Office of Science, Biological and Environmental Research under contract DE-AC05-00OR22725. Oak Ridge National Laboratory is managed by UT-Battelle, LLC for the United States Department of Energy.

References

Aber, J. D., and J. M. Melillo (1980), Litter decomposition: Measuring state of decay and percent transfer into forest soils, *Can. J. Bot.*, *58*, 416–421.

Ahmad, R., R. S. Kookana, A. M. Alston, and J. O. Skjemstad (2001), The nature of soil organic matter affects sorption of pesticides. 1. Relationships with carbon chemistry as determined by 13C CPMAS NMR spectroscopy, *Environ. Sci. Technol.*, *35*, 878–884.

Aravena, R., B. G. Warner, D. J. Charman, L. R. Belyea, S. P. Mathur, and H. Dinel (1993), Carbon isotopic composition of deep carbon gases in an ombrogenous peatland, northwestern Ontario, Canada, *Radiocarbon*, *35*, 271–276.

Artz, R. R. E., S. J. Chapman, A. H. J. Robertson, J. M. Potts, F. Laggoun-Défarge, S. Gogo, L. Comont, J. R. Disnar, and A. J. Francez (2008), FTIR spectroscopy can be used as a screening tool for organic matter quality in regenerating cutover peatlands, *Soil Biol. Biochem.*, *40*, 515–527.
Asada, T., B. Warner, and R. Aravena (2005), Effects of the early stage of decomposition on change in carbon and nitrogen isotopes in *Sphagnum* litter, *J. Plant Interact.*, *1*, 229–237.
Baldock, J. A., and C. M. Preston (1995), Chemistry of carbon decomposition processes in forests as revealed by solid-state carbon-13 nuclear magnetic resonance, in *Carbon Forms and Functions in Forest Soils*, pp. 89–117, Madison, Wis.
Baldock, J. A., J. M. Oades, D. J. Nelson, T. M. Skene, A. Golchin, and P. Clarke (1997), Assessing the extent of decomposition of natural organic materials using solid-state ^{13}C NMR spectroscopy, *Aust. J. Soil Res.*, *35*, 1061–1083.
Beer, J., K. Lee, M. Whiticar, and C. Blodau (2008), Geochemical controls on anaerobic organic matter decomposition in a northern peatland, *Limnol. Oceanogr.*, *53*, 1393–1407.
Benner, R., M. L. Fogel, E. K. Sprague, and R. E. Hodson (1987), Depletion of ^{13}C in lignin and its implications for stable carbon isotope studies, *Nature*, *329*, 708–710.
Borgmark, A., and K. Schoning (2006), A comparative study of peat proxies from two eastern central Swedish bogs and their relation to meteorological data, *J. Quat. Sci.*, *21*, 109–114.
Broder, T., C. Blodau, H. Biester, and K. H. Knorr (2012), Peat decomposition records in three pristine ombrotrophic bogs in southern Patagonia, *Biogeosciences*, *9*, 1479–1491.
Chanton, J. P., J. E. Bauer, P. A. Glaser, D. I. Siegel, C. A. Kelley, S. C. Tyler, E. H. Romanowicz, and A. Lazrus (1995), Radiocarbon evidence for the substrates supporting methane formation within northern Minnesota peatlands, *Geochim. Cosmochim. Acta*, *59*, 3663–3668.
Chanton, J. P., P. H. Glaser, L. S. Chasar, D. J. Burdige, M. E. Hines, D. I. Siegel, L. B. Tremblay, and W. T. Cooper (2008), Radiocarbon evidence for the importance of surface vegetation on fermentation and methanogenesis in contrasting types of boreal peatlands, *Global Biogeochem. Cycles*, *22*, GB4022, doi:10.1029/2008GB003274.
Chapman, S. J., C. D. Campbell, A. R. Fraser, and G. Puri (2001), FTIR spectroscopy of peat in and bordering Scots pine woodland: Relationships with chemical and biological properties, *Soil Biol. Biochem.*, *33*, 1193–1200.
Charman, D. J., R. Aravena, and B. G. Warner (1994), Carbon dynamics in a forested peatland in north-eastern Ontario, Canada, *J. Ecol.*, *82*, 55–62.
Charman, D. J., R. Aravena, C. L. Bryant, and D. D. Harkness (1999), Carbon isotopes in peat, DOC, CO2, and CH4 in a Holocene peatland on Dartmoor, southwest England, *Geology*, *27*, 539–542.
Chasar, L. S., J. P. Chanton, P. H. Glaser, D. I. Siegel, and J. S. Rivers (2000), Radiocarbon and stable carbon isotopic evidence for transport and transformation of dissolved organic carbon, dissolved inorganic carbon, and CH4 in a northern Minnesota peatland, *Global Biogeochem. Cycles*, *14*, 1095–1108.
Christensen, T. R., A. Michelsen, S. Jonasson, and I. K. Schmidt (1997), Carbon dioxide and methane exchange of a subarctic heath in response to climate change related environmental manipulations, *Oikos*, *79*, 34–44.
Christensen, T. R., N. Panikov, M. Mastepanov, A. Joabsson, A. Stewart, M. Oquist, M. Sommerkorn, S. Reynaud, and B. Svensson (2003), Biotic controls on CO2 and CH4 exchange in wetlands—A closed environment study, *Biogeochemistry*, *64*, 337–354.
Clymo, R. S. (1984), The limits to peat bog growth, *Philos. Trans. R. Soc. B*, *303*, 605–654.
Clymo, R. S., and C. L. Bryant (2008), Diffusion and mass flow of dissolved carbon dioxide, methane, and dissolved organic carbon in a 7-m deep raised peat bog, *Geochim. Cosmochim. Acta*, *72*, 2048–2066.
Cocozza, C., V. D'Orazio, T. M. Miano, and W. Shotyk (2003), Characterization of solid and aqueous phases of a peat bog profile using molecular fluorescence spectroscopy, ESR and FT-IR, and comparison with physical properties, *Org. Geochem.*, *34*, 49–60.
Conant, R. T., et al. (2011), Temperature and soil organic matter decomposition rates—Synthesis of current knowledge and a way forward, *Global Change Biol.*, *17*, 3392–3404.
Corbett, J. E., M. M. Tfaily, D. J. Burdige, W. T. Cooper, P. H. Glaser, and J. P. Chanton (2013a), Partitioning pathways of CO_2 production in peatlands with stable carbon isotopes, *Biogeochemistry*, *114*, 327–340.
Corbett, J. E., D. J. Burdige, M. M. Tfaily, A. R. Dial, W. T. Cooper, P. H. Glaser, and J. P. Chanton (2013b), Surface production fuels deep heterotrophic respiration in northern peatlands, *Global Biogeochem. Cycles*, *27*, 1163–1174, doi:10.1002/2013GB004677.
Dai, J., M.-Y. Sun, R. A. Culp, and J. E. Noakes (2005), Changes in chemical and isotopic signatures of plant materials during degradation: Implication for assessing various organic inputs in estuarine systems, *Geophys. Res. Lett.*, *32*, L13608, doi:10.1029/2005GL023133.
Damman, A. W. H. (1988), Regulation of nitrogen removal and retention in Sphagnum bogs and other peatlands, *Oikos*, *51*, 291–305.
Ekono (1981), Report on energy use of peat, Contribution to U.N. Conference on New and Renewable Sources of Energy, Nairobi.
Franzén, L. G. (2006), Increased decomposition of subsurface peat in Swedish raised bogs: Are temperate peatlands still net sinks of carbon?, *Mires Peat*, *1*, Article 3.
Freeman, C., N. Ostle, and H. Kang (2001), An enzymic 'latch' on a global carbon store, *Nature*, *409*, 149.
Fründ, R., G. Guggenberger, K. Haider, H. Knicker, I. Kögel-Knabner, H.-D. Lüdemann, J. Luster, W. Zech, and M. Spiteller (1994), Recent advances in the spectroscopic characterization of soil humic substances and their ecological relevance, *Z. Pflanzenernaehr. Bodenkd.*, *157*, 175–186.
Ghosh, P., and W. A. Brand (2003), Stable isotope ratio mass spectrometry in global climate change research, *Int. J. Mass Spectrom.*, *228*, 1–33.
Hamdan, R., H. M. El-Rifai, A. W. Cheesman, B. L. Turnere, K. R. Reddy, and W. T. Cooper (2012), Linking phosphorus sequestration to carbon humification in wetland soils by 31P and 13C NMR spectroscopy, *Environ. Sci. Technol.*, *46*(9), 4775–4782.
Hertkorn, N., A. Permin, I. Perminova, D. Kovalevskii, M. Yudov, V. Petrosyan, and A. Kettrup (2002), Comparative analysis of partial structures of a peat humic and fulvic acid using one- and two-dimensional nuclear magnetic resonance spectroscopy, *J. Environ. Qual.*, *31*, 375–387.
Holden, J. (2005), Peatland hydrology and carbon release: Why small-scale process matters, *Philos. Trans. R. Soc. A*, *363*, 2891–2913.
Holmgren, A., and B. Nordén (1988), Characterization of peat samples by diffuse reflectance FT-IR spectroscopy, *Appl. Spectrosc.*, *42*, 255–262.
Hopkins, D. W., J. A. Chudek, E. A. Webster, and D. Barraclough (1997), Following the decomposition of ryegrass labelled with ^{13}C and ^{15}N in soil by solid-state nuclear magnetic resonance spectroscopy, *Eur. J. Soil Sci.*, *48*, 623–631.
Hornibrook, E. R. C., F. J. Longstaffe, and W. S. Fyfe (1997), Spatial distribution of microbial methane production pathways in temperate zone wetland soils: Stable carbon and hydrogen isotope evidence, *Geochim. Cosmochim. Acta*, *61*, 745–753.
Jackson, L. E., J. P. Schimel, and M. K. Firestone (1989), Short-term partitioning of ammonium and nitrate between plants and microbes in an annual grassland, *Soil Biol. Biochem.*, *21*, 409–415.
Kalbitz, K., S. Solinger, J. H. Park, B. Michalzik, and E. Matzner (2000), Controls on the dynamics of dissolved organic matter in soils: A review, *Soil Sci.*, *165*, 277–304.
Keough, J. R., C. A. Hagley, E. Ruzycki, and M. Sierszen (1998), ^{13}C composition of primary producers and role of detritus in a freshwater coastal ecosystem, *Limnol. Oceanogr.*, *43*, 734–740.
Klavins, M., J. Sire, O. Purmalis, and V. Melecis (2008), Approaches to estimating humification indicators for peat, *Mires Peat*, *3*, Article 7.

Koarashi, J., T. Iida, and T. Asano (2005), Radiocarbon and stable carbon isotope compositions of chemically fractionated soil organic matter in a temperate-zone forest, *J. Environ. Radioact.*, *79*, 137–156.
Kögel-Knabner, I. (2000), Analytical approaches for characterizing soil organic matter, *Org. Geochem.*, *31*, 609–625.
Kolka, R. (2011), *Peatland Biogeochemistry and Watershed Hydrology at the Marcell Experimental Forest*, CRC Press, Boca Raton.
Kramer, M. G., P. Sollins, R. S. Sletten, and P. K. Swart (2003), N isotope fractionation and measures of organic matter alteration during decomposition, *Ecology*, *84*, 2021–2025.
Kuhry, P., and D. H. Vitt (1996), Fossil carbon/nitrogen ratios as a measure of peat decomposition, *Ecology*, *77*, 271–275.
Leifeld, J., M. Steffens, and A. Galego-Sala (2012), Sensitivity of peatland carbon loss to organic matter quality, *Geophys. Res. Lett.*, *39*, L14704, doi:10.1029/2012GL051856.
Limpens, J., F. Berendse, C. Blodau, J. G. Canadell, C. Freeman, J. Holden, N. Roulet, H. Rydin, and G. Schaepman-Strub (2008), Peatlands and the carbon cycle: From local processes to global implications—A synthesis, *Biogeosciences*, *5*, 1475–1739.
Lucas, R. E. (1982), *Organic Soils (Histosols): Formation, Distribution, Physical and Chemical Properties and Management for Crop Production*, 77 pp., Michigan State Univ., Farm Science Research Report 435, Michigan.
Lützow, M. v., I. Kögel-Knabner, K. Ekschmitt, E. Matzner, G. Guggenberger, B. Marschner, and H. Flessa (2006), Stabilization of organic matter in temperate soils: Mechanisms and their relevance under different soil conditions—A review, *Eur. J. Soil Sci.*, *57*, 426–445.
Moore, T., and N. Basiliko (2006), Decomposition in boreal peatlands, in *Boreal Peatland Ecosystems*, Springer, Berlin, Heidelberg, pp. 125–143.
Nichols, D. S., and J. M. Brown (1980), Evaporation from a *Sphagnum* moss surface, *J. Hydrol.*, *48*, 289–302.
Preston, C. M. (1996), Applications of NMR to soil organic matter analysis: History and prospects, *Soil Sci.*, *161*(3), 144–166.
Preston, C. M., P. F. Centre, A. C. M. Rusk (1990), A Bibliography of NMR Applications for Forestry Research. Forestry Canada, *Information Report BC-X-322*, 49 pp., Pacific Forestry Centre, Victoria, BC.
Schnitzer, M. (1991), Soil organic matter—The next 75 years, *Soil Sci.*, *151*, 41–58.
Sebestyen, D. S., C. Dorrance, D. M. Olson, E. S. Verry, R. K. Kolka, A. E. Elling, and R. Kyllander (2011), Long-term monitoring site and trends at the Marcell Experimental Forest, in *Peatland Biogeochemistry and Watershed Hydrology at the Marcell Experimental Forest*, pp. 93–134, CRC Press, Boca Raton, Fla.
Segnini, A., A. A. de Souza, E. H. Novotny, D. M. B. P. Milori, W. T. L. da Silva, T. J. Bonagamba, A. Posadas, and R. Quiroz (2013), Characterization of peatland soils from the high Andes through ^{13}C nuclear magnetic resonance spectroscopy, *Soil Sci. Soc. Am. J.*, *77*, 673–679.
Siegel, D. I., A. S. Reeve, P. H. Glaser, and E. A. Romanowicz (1995), Climate-driven flushing of pore water in peatlands, *Nature*, *374*, 531–533.
Sjögersten, S., B. L. Turner, N. Mahieu, L. M. Condron, and P. A. Wookey (2003), Soil organic matter biochemistry and potential susceptibility to climatic change across the forest-tundra ecotone in the Fennoscandian mountains, *Global Change Biol.*, *9*, 759–772.
Taylor, A. F. S., P. M. Fransson, P. Högberg, M. N. Högberg, and A. H. Plamboeck (2003), Species level patterns in ^{13}C and ^{15}N abundance of ectomycorrhizal and saprotrophic fungal sporocarps, *New Phytol.*, *159*, 757–774.
Turunen, J., E. Tomppo, K. Tolonen, and A. Reinikainen (2002), Estimating carbon accumulation rates of undrained mires in Finland—Application to boreal and subarctic regions, *Holocene*, *12*, 69–80.
Urban, N. R., S. J. Eisenreich, and D. F. Grigal (1989), Sulfur cycling in a forested *Sphagnum* bog in northern Minnesota, *Biogeochemistry*, *7*, 81–109.
Vardy, S. R., B. G. Warner, J. Turunen, and R. Aravena (2000), Carbon accumulation in permafrost peatlands in the Northwest Territories and Nunavut, Canada, *Holocene*, *10*, 273–280.
Verry, E. S. (1981), Water table and streamflow changes after stripcutting and clearcutting an undrained black spruce bog, in *Proceedings of the Sixth International Peat Congress, Duluth, MN, August 17–23, 1980*, W.A. Fisher Company, Eveleth, MN, pp. 493–498.
Waksman, S. A. (1924), Influence of microorganisms upon the carbon–nitrogen ratio in the soil, *J. Agric. Sci.*, *14*, 555–562.
Waksman, S. A., and F. G. Tenney (1927), The composition of natural organic materials and their decomposition in the soil: II. Influence of age of plant upon the rapidity and nature of its decomposition-rye plants, *Soil Sci.*, *24*, 317–334.
Wang, G. A., X. H. Feng, J. M. Han, L. Zhou, W. Tan, and F. Su (2008), Paleovegetation reconstruction using $\delta^{13}C$ of soil organic matter, *Biogeosciences*, *5*, 1325–1337.
Williams, C. J., and J. B. Yavitt (2003), Botanical composition of peat and degree of peat decomposition in three temperate peatlands, *Ecoscience*, *10*, 85–95.
Williams, R. T., and R. L. Crawford (1984), Methane production in Minnesota peatlands, *Appl. Environ. Microbiol.*, *47*, 1266–1271.
Wilson, M. A., P. F. Barron, and A. H. Gillam (1981), The structure of freshwater humic substances as revealed by ^{13}C-NMR spectroscopy, *Geochim. Cosmochim. Acta*, *45*, 1743–1750.